

# Growth of 'dizzy dendrites' in a random field of foreign particles

LÁSZLÓ GRÁNÁSY\*<sup>1</sup>, TAMÁS PUSZTAI<sup>1</sup>, JAMES A. WARREN<sup>2</sup>, JACK F. DOUGLAS<sup>3</sup>, TAMÁS BÖRZSÖNYI<sup>1</sup> AND VINCENT FERREIRO<sup>4</sup>

<sup>1</sup>Research Institute for Solid State Physics and Optics, PO Box 49, H-1525 Budapest, Hungary

<sup>2</sup>Metallurgy and <sup>3</sup>Polymers Divisions, National Institute of Standards and Technology, Gaithersburg, Maryland 20899, USA

<sup>4</sup>Laboratoire de Structure et Propriétés de l'Etat Solide, CNRS, Batiment C6, 59655 Villeneuve d'Ascq, France

\*e-mail: grana@szfki.hu

Published online: 19 January 2003; doi:10.1038/nmat815

**M**icrostructure plays an essential role in determining the properties of crystalline materials<sup>1</sup>. A widely used method to influence microstructure is the addition of nucleating agents<sup>1</sup>. Observations on films formed from clay–polymer blends indicate that particulate additives, in addition to serving as nucleating agents, may also perturb crystal growth, leading to the formation of irregular dendritic morphologies<sup>2,3</sup>. Here we describe the formation of these 'dizzy dendrites' using a phase-field theory, in which randomly distributed foreign particle inclusions perturb the crystallization by deflecting the tips of the growing dendrite arms. This mechanism of crystallization, which is verified experimentally, leads to a polycrystalline structure dependent on particle configuration and orientation. Using computer simulations we demonstrate that additives of controlled crystal orientation should allow for a substantial manipulation of the crystallization morphology.

A hallmark of materials technology is the engineering of materials with crystalline microstructure suitable for applications ranging from microelectronics to turbine blades<sup>1</sup>. Under almost all relevant casting circumstances, alloys solidify dendritically (that is, with the snowflake or arboresque morphology characterized by its multilevel branching as exemplified in Fig. 1)<sup>1</sup>. This complex morphology reflects a competition between order associated with the symmetries of the crystal structure and morphological instabilities arising from the nonlinear transport processes. The presence of additives or small 'heterogeneities' in the non-equilibrium melt provides a source of randomness that can potentially influence the large-scale crystallization structure. It has long been suggested that microscopic impurities may be responsible for a transition between regular dendritic growth of single crystals and polycrystalline crystal morphologies. The densely branched spherulite crystal morphology, found ubiquitously in polymer materials, has been argued to have this generic origin<sup>4</sup>. Experiments on films formed from clay–polymer blends<sup>2,3</sup> indicate that the effect of foreign particles on the growing dendritic crystals is fairly complex. Whereas regular dendritic patterns form in the absence of clay particles, disordered dendritic morphologies appear at high clay concentrations (Fig. 2). (For all experimental dendrites shown, the concentration of the PEO to PMMA is 70/30 by relative polymer mass in the polymer solutions in which the films were cast.) The dendrite trunks exhibit a tendency towards

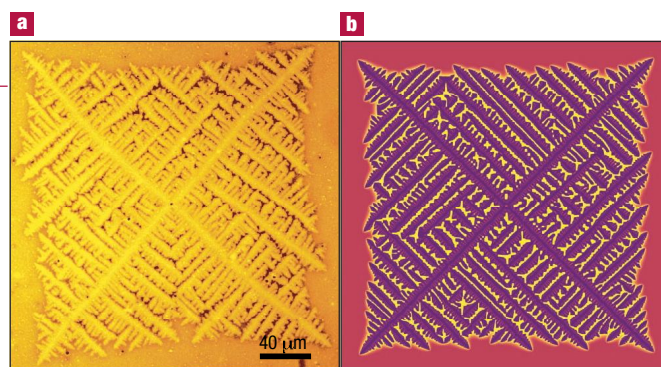


**Figure 1** Experimental versus simulated dendrites. **a**, Image of a PEO/PMMA dendrite taken by Nikon optical microscope. Black and white image has been rendered in false colour to provide better contrast. **b**, Ni/Cu dendrite simulated on a  $2,000 \times 2,000$  grid ( $26.3 \mu\text{m} \times 26.3 \mu\text{m}$ ) using an anisotropy of  $\epsilon = 0.25$ . Note, that the difference in the size scales originates from the different physical properties of the Ni/Cu and polymer systems and from the larger supersaturation used to speed up the computations. (On the right a composition map is shown. Continuous variation of colour between purple and yellow indicates a variation of the local composition between the solidus and liquidus compositions.)

'curling', and extra arms appear that do not match the initial orientation of the crystal. The mechanism by which these irregular patterns form has not yet been identified.

Herein, we use the phase-field method<sup>5–9</sup> to explore how the foreign particles modify the nature of dendritic growth, and compare the results with further experiments on clay–polymer blend films. We show that an interaction between dendrite tips and foreign particles is responsible for the appearance of 'dizzy dendrites', which are polycrystalline structures formed by sequential deflection of the dendrite tip on clay particles, a mechanism that can be exploited to control solidification microstructures.

Preparation of the clay-filled polyethylene oxide (PEO) (Aldrich) and polymethyl methacrylate (PMMA) (Aldrich) blend films has been described previously<sup>2,3</sup>. Briefly, we used 'cloisite' clay (Southern Clay Products), which we organically modified with surfactant



**Figure 2** 'Dizzy' dendrites. **a,b**, Growth shapes formed in 80-nm-thick films of a clay-PEO/PMMA blend with 15% relative mass of clay to polymer. **c**, Composition map from a phase-field simulation on a  $3,000 \times 3,000$  grid ( $39.4 \mu\text{m} \times 39.4 \mu\text{m}$ ) using 18,000 single-pixel orientation-pinning centres distributed randomly. (The same scale applies for **a** and **b**.)

(distearyl dimethyl ammonium chloride) to make it more compatible with the PEO/PMMA blend. Solutions of the polymer blend and clay were prepared in chloroform and then spun-cast onto smooth, acid-cleaned Si substrates. This procedure resulted in uniform films having a thickness ranging between 50 nm and 500 nm, depending on the spin-casting speed. (The films were chosen to be very thin so that the crystallization process should be close to two-dimensional.) After spin-casting, the films were heated to 377 K (above the PEO melting temperature of 338 K) for 10 min, to melt the crystal structures formed during the casting process. Reflective optical images of the crystallization patterns were made with an optical microscope with a CCD camera attachment. The clay particles are roughly spherical and comprise stacks of mica sheets so that they are presumably flat at a molecular scale. The particle orientation is associated with the sheet-stacking direction. Tunnelling electron microscope images indicate that the sizes of these clay particles and particle clusters range from 10 nm to  $1 \mu\text{m}$ . The limited film thickness constrains the range of particle size that we can investigate. Experimental techniques are as yet unable to

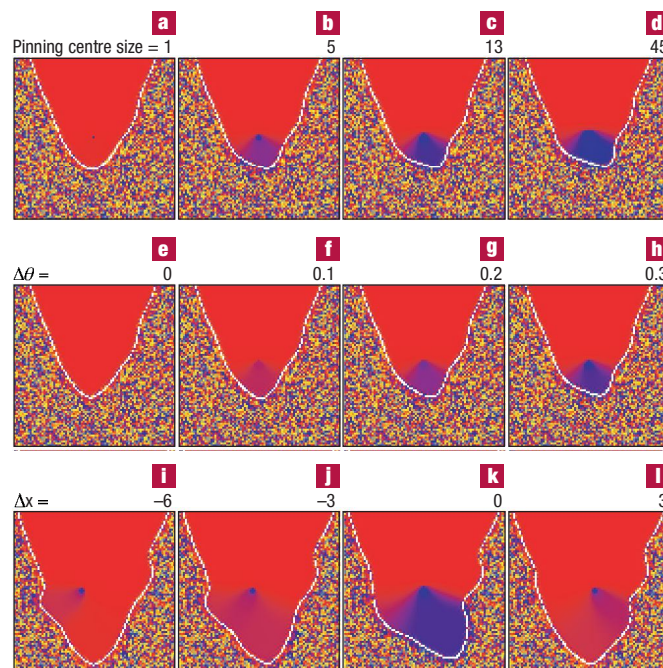


**Figure 3** Interaction of pinning centres with a dendrite tip of initial orientation,  $\theta = 0$  (fast growth direction is downwards). The blue regions in the solid evince the formation of a region with a new orientation (and growth direction). **a–d**, The effect of the size of the pinning centre (in pixels) at constant orientation mismatch ( $\Delta\theta = 1/3$ ). The tip deflection increases with size. **e–f**, The effect of a difference in orientation,  $\Delta\theta$ , for pinning centres of constant size (13 pixels). The tip deflection increases with  $\Delta\theta$ . **i–l**, The effect of lateral displacement,  $\Delta x$  (in pixels), for five-pixel pinning centres of  $\Delta\theta = 1/3$ . The tip deflection decreases with increasing  $|\Delta x|$ . The different colours in the orientation map denote different crystal orientations on a continuous scale that assigns red, blue, grey, and yellow for  $\theta = 0, 1/3, 1/2$ , and  $2/3$ . Note the random orientation in liquid. (See the randomly coloured pixels around the red/blue dendrite.) The white contour denotes the solidification front,  $\theta = 1/2$ . The anisotropy,  $\epsilon$ , used in the simulations was 0.05.

resolve the layering direction of the clay sheets within each individual particle. It appears that only a small fraction of the clay particles influence the growth morphology.

The particle-induced morphological changes were modelled using a phase-field theory<sup>5,6</sup> that incorporates the nucleation of crystals with different crystallographic orientations. This approach is based on previous developments for binary solidification<sup>7</sup> and multigrain growth<sup>8,9</sup>. The local physical state is characterized by a structural order parameter  $\phi$  (phase field) that describes the liquid–crystal transition, the chemical composition, and an orientation field  $\theta$ . The field  $\theta$  specifies the crystal orientation in the laboratory frame<sup>8,9</sup>. This variable captures the feature that the short-range order in the solid and liquid is usually similar, and can therefore be represented by a local value of  $\theta$ . The free energy,  $F$ , is given by the integral,  $F = \int dr \{ \alpha^2 T |\nabla\phi|^2 + f + f_{\text{ori}} \}$ , where  $\alpha$  is a constant and  $T$  the temperature. The square-gradient term  $|\nabla\phi|^2$  ensures a diffuse crystal–liquid interface, seen in experiment<sup>10</sup> and computer simulations<sup>11,12</sup>. The local free energy  $f$  has two minima whose relative depth is the driving force for crystallization, and is a function of both temperature and composition. The orientation contribution to the free energy  $f_{\text{ori}} = M(\phi) |\nabla\theta|^2$  represents the excess free energy due to inhomogeneities in crystal orientation in space, in particular the misorientation due to a grain boundary<sup>5,6,8,9</sup>.  $M$  is an interpolating function from the solid and the liquid. The form of  $f_{\text{ori}}$  ensures that  $\theta$  takes an essentially constant value (scaled between 0 and 1) in the solid, whereas it fluctuates in the liquid<sup>5,6</sup>. The orientational ordering takes

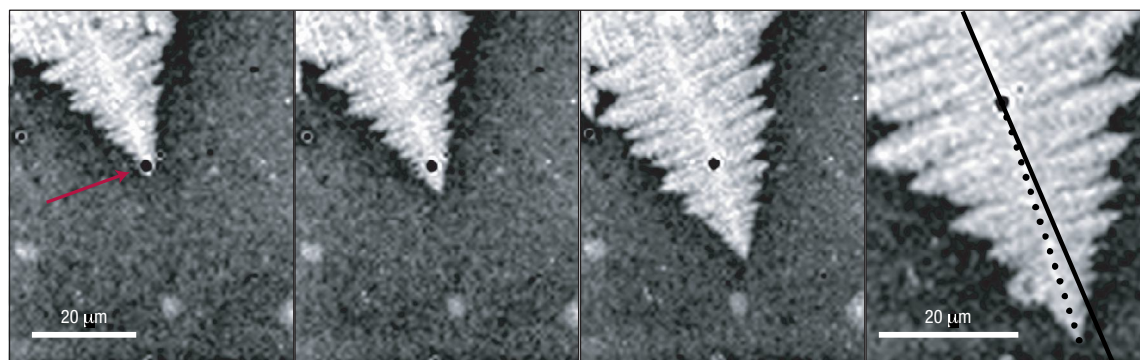


**Figure 4** Sequence of snapshots taken by optical microscope that shows the engulfment of a clay particle (dark spot marked by red arrow) by the advancing PEO dendrite. Note the deflection of the dendrite tip after impingement. The solid and dotted lines in the panel on the far right show the original and deflected growth directions of the dendrite tip, respectively. The scales are the same for the three images on the left, and a different scale applies to the image on the far right.

place at the diffuse interface simultaneously with the structural transition. The time evolution is governed by relaxational dynamics and Langevin noise terms.

Engulfment of a clay particle into the advancing PEO dendrite is a complex phenomenon. The optimum alignment of a clay particle depends on the anisotropy, of the clay–PEO interface free energy and the shape of the particle. Deviation from this optimum alignment would force the growing crystal to build high-energy interfaces. At low growth rates this might be prevented by particle rotation/pushing<sup>13</sup>. At high rates (as in our case), the system might reduce its free energy by forming new grains. This phenomenon is driven by the impetus to reduce the crystallographic misfit along the PEO–clay perimeter by creating grain boundaries within the PEO crystal, a process that may change the crystal orientation at the dendrite tip, thus changing the tip trajectory ('tip deflection'). Neglecting differences in composition and crystal structure, and assuming that the only source of the clay–PEO interface free energy is the orientation misfit between the clay particle and PEO dendrite, we introduce the possible, simplest representation of the clay particles. Along this line, we insert randomly distributed 'orientation pinning centres' into the simulation, which are represented by regions of externally imposed orientation.

Because relevant material properties are unknown for the PEO/PMMA mixtures, the computations were performed for the familiar Ni/Cu system, which, as in the case of PEO/PMMA, crystallizes as dendrites with fourfold-symmetry under far from equilibrium conditions. The simulations were done at a temperature below the melting point of pure Ni and above the melting point of pure Cu (PEO crystallizes upon cooling, but PMMA remains amorphous). Because the growing tips of the polymer dendrites (see Fig. 1 and ref. 14) are rather sharp, we assume a large (arbitrary in the absence of direct measurement) anisotropy ( $\epsilon$ ) and a symmetry ( $m$ ) consistent with these patterns. Specifically, we assume large ( $\epsilon = 0.25$ ) fourfold ( $m = 4$ ) anisotropy for the solid–liquid interface free energy,  $\gamma = \gamma_0 \{1 + \epsilon \cos[m(\psi - \theta)]\}$ , where  $\psi$  is the inclination of the liquid–solid interface in the laboratory frame and  $\gamma_0$  is the mean surface energy.

The dendrites that form in experiment and simulation compare well for the case when no foreign particles are present (Fig. 1), as discussed further elsewhere<sup>3</sup>. Moreover, we find that tip deflection happens only when the pinning centre is above a critical size (Fig. 3). With increasing anisotropy the dendrite tip becomes sharper, and the critical size decreases. Indeed, for  $\epsilon > 1/15$  the tip radius is effectively one pixel due to the presence of missing orientations in the growth

direction<sup>15</sup>. Thus, we find that for  $\epsilon = 0.25$  even single pixels are able to deflect the dendrite tip. A preliminary study of impingement at lower anisotropies ( $\epsilon = 0.03$ ) suggests that the critical deflection size scales with the tip radius  $R$  (a critical radius of approximately  $R/4$ ). Pinning centres cause deflection only if directly hit by the dendrite tip, a finding confirmed by our experimental observations (Fig. 4). This explains why only a small fraction of the pinning centres influence morphology. The deflection angle increases both with the size of the pinning centre, and its misorientation to the axis of the impinging dendrite.

Using an appropriate density of single-pixel pinning centres (18,000 per frame, which is comparable to the number of  $\sim 1 \mu\text{m}$  size particles estimated for Fig. 2), we obtain a striking similarity between experiment and simulation (Fig. 2). This extends to such details as curling of the main arms and the appearance of extra arms. This disorder in dendrite morphology is due to the multigrain (polycrystalline) structure (Fig. 5) that develops during a sequential deflection of dendrite tips on orientation pinning centres (clay particles). The curling effect has its origin in the interaction between the dendrite arms generated through the side branches (K. Lee & W. Losert, unpublished results). The argument is as follows: suppose that a fluctuation in particle density deflects the tip of a dendrite trunk and that this tip is also somewhat further out than the other trunk tips. The interaction between the side branches causes the other trunks to deflect in the same direction, leading to a cascade of deflections. This spontaneous symmetry breaking yields a vortex-like crystallization pattern similar to perturbed reaction–diffusion fronts<sup>3</sup>. If the deflected tip is not 'out front' or if there are competing deflections of comparable strength, then the deflection process becomes less coherent and a random branching process (meandering dendrite) is obtained.

An intriguing question is whether this mechanism could be exploited to control solidification morphologies and microstructure. As might be expected, if we assign the same orientation to all the pinning centres, whether distributed randomly or on triangular/square lattices, the dendrite arms bend so that their final crystallographic orientation coincides with that of the pinning centres. Other interesting possibilities are the presence of pinning lines and uniformly rotating pinning centres. Parallel pinning lines of alternating orientation lead to zigzagging dendrite arms and a striped orientation map, whereas the rotating pinning centres (randomly distributed or on a lattice) lead to spiralling dendrites (Fig. 6). Experimental realization of these complex pinning conditions is certainly a challenge. Possible control methods might include the use of substrate-embedded oriented particles,

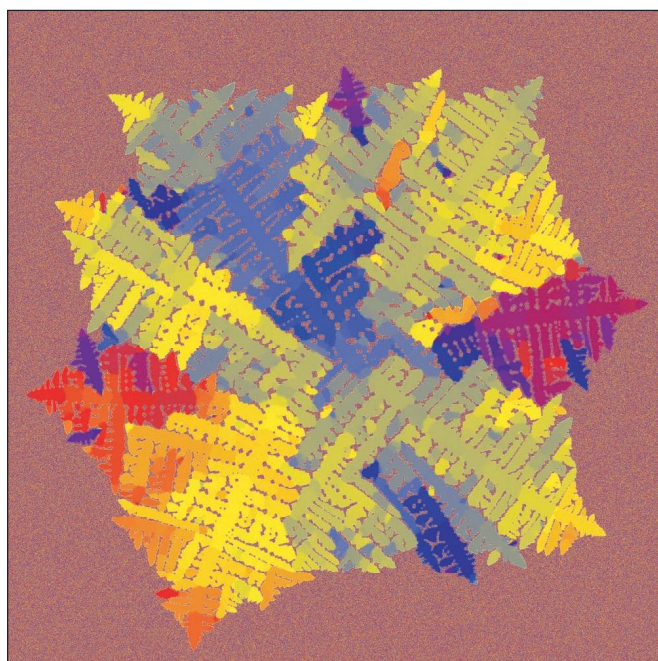


**Figure 5** Orientation map for the 'dizzy' dendritic particle from simulation shown in Fig. 2. Note the polycrystalline structure. Different colours stand for different crystal orientations. (Colouring is the same as for Fig. 3.)

the rotation of an external electromagnetic field, or angular momentum control by laser pulses<sup>16</sup>. Previous work has shown that particles are not necessary to nucleate crystallization in the thin polymer films, and that nucleation can be achieved by simply piercing the film with a sharp glass fibre (W. Losert, unpublished work). By extension, it should be possible to print arrays of nucleation sites with specified symmetry of configuration by simply rolling a cylinder with an array of asperities over the uncrystallized polymer film, as in printing patterns on a pie crust. The orientation of nucleation points could be controlled by making the asperities in the form of flat pins with controlled orientation. In this way, it should be possible to create a wide range of crystallization morphologies and to tune the topography, permeability and the mechanical properties of the crystallized polymer film. Such orientation-controlling techniques may open a new route for tailoring solidification microstructures.

We note that previous observations on small molecular organic liquids (for example, succinonitrile) and metal alloys (Al–Cu) have indicated the propensity of 'fine particles' (of the order of the size of the dendrite tip or smaller) to cause the dendrite tips to split if the crystallization rate is sufficiently high to engulf the particles<sup>17,18</sup>. The fine particles are incorporated rather uniformly into the crystallization pattern at high rates of crystallization, but tend to be pushed by the front at lower rates. Kinetic factors as well as equilibrium energy factors seem to be important for particle engulfment<sup>13,17–20</sup>. Notably, these former studies have not shown a tendency for the particles to nucleate new fronts with a different crystallographic orientation. Future studies should explore whether highly anisotropic particles (for example, fibres) can effectively transform metallurgical crystallization fronts into polycrystalline structures similar to those seen in our simulations and the film measurements of polymer blends.

Clearly, both the particle engulfment and deflection process depend on the interaction of the particles with factors such as the crystallizing matrix, particle shape, particle concentration, crystallization pattern

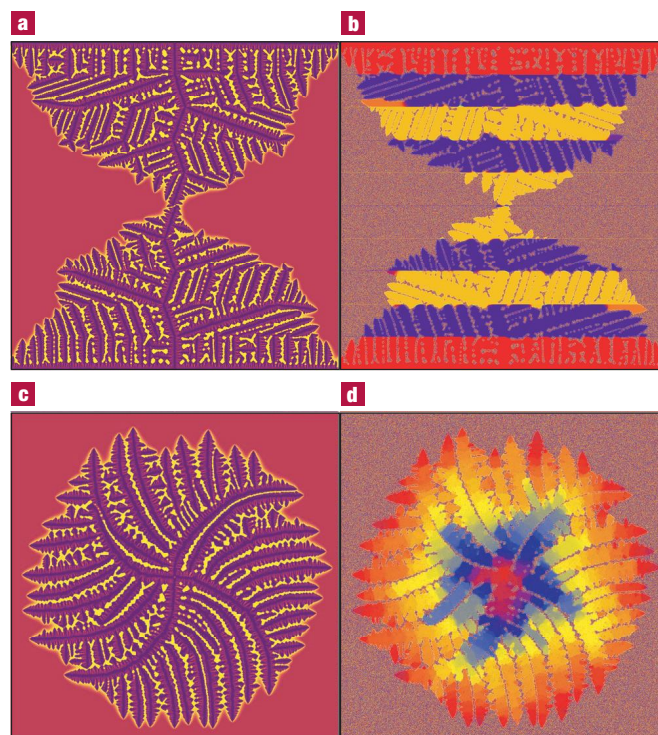


**Figure 6** Phase-field simulations for complex pinning conditions. **a**, Parallel pinning lines with alternating orientation, shown in the composition map, yield the striped orientation map in **b**. **c**, Randomly distributed but uniformly rotating orientation pinning centres lead to the spiralling dendrites in **d**. Computations were performed on  $1,800 \times 1,800$  ( $23.6 \mu\text{m} \times 23.6 \mu\text{m}$ ) (**a,b**) and  $1,500 \times 1,500$  grids ( $19.7 \mu\text{m} \times 19.7 \mu\text{m}$ ) (**c,d**).

type (such as seaweed, dendrite and spherulite). Quantitative changes in the geometry of the growing crystallization patterns should therefore be investigated in future work. We expect the phenomena to be quite rich, but the general feature of the formation of highly disordered, branched crystal patterns with a concentration of particles, as found in the present paper, is expected to be general.

In summary, these findings broaden our understanding of the disordered morphology realized in crystallization patterns found in systems with appreciable amounts of particulate impurities—a common situation in real materials. Manipulation of both the configuration and orientation of the nucleating particles should allow for substantial control of the large-scale crystallization morphology for many applications.

Received 3 October 2002; accepted 16 December 2002; published 19 January 2003.

#### References

1. Cahn, R. W. *The Coming of Materials Science* (Pergamon, Oxford, 2001).
2. Ferreiro, V., Douglas, J. F., Warren, J. A. & Karim, A. Nonequilibrium pattern formation in the crystallization of polymer blend films. *Phys. Rev. E* **65**, 042802 (2002).
3. Ferreiro, V., Douglas, J. F., Warren, J. A. & Karim, A. Growth pulsations in symmetric dendritic crystallization in polymer blend films. *Phys. Rev. E* **65**, 051606 (2002).
4. Keith, H. D. & Padden, F. J. Crystallization of polymers from the melt and the structure of bulk semicrystalline polymers. *J. Appl. Phys.* **34**, 2409–2421 (1963).
5. Gránásy, L., Börzsönyi, T. & Pusztai, T. Nucleation and bulk crystallization in binary phase field theory. *Phys. Rev. Lett.* **88**, 206105 (2002).
6. Gránásy, L., Börzsönyi, T. & Pusztai, T. Crystal nucleation and growth in binary phase field theory. *J. Cryst. Growth* **237–239**, 1813–1817 (2002).
7. Warren, J. A. & Boettinger, W. J. Prediction of dendritic growth and microsegregation patterns in a binary alloy using the phase-field method. *Acta Metall. Mater.* **43**, 689–703 (1995).
8. Kobayashi, R., Warren, J. A. & Carter, W. C. Vector-valued phase field model for crystallization and grain boundary formation. *Physica D* **119**, 415–423 (1998).

9. Kobayashi, R., Warren, J. A. & Carter, W. C. Modeling grain boundaries using a phase-field technique. *Physica D* **140**, 141–150 (2000).
10. Huisman, W. J. *et al.* Layering of a liquid metal in contact with a hard wall. *Nature* **390**, 379–381 (1997).
11. Davidchack, R. L. & Laird, B. B. Simulation of the hard-sphere crystal-melt interface. *J. Chem. Phys.* **108**, 9452–9462 (1998).
12. Hoyt, J. J., Asta, M. & Karma, A. Method for computing the anisotropy of the solid-liquid interfacial free energy. *Phys. Rev. Lett.* **86**, 5530–5533 (2001).
13. Stefanescu, D. M., Moitra, A., Kacar, A. S. & Dhindaw, B. K. The influence of buoyant forces and volume fraction of particles on the particle pushing/entrapment transition during directional solidification of Al/SiC and Al/graphite composites. *Metall. Trans. A* **29**, 231–239 (1990).
14. Magill, J. H. Spherulites: A personal perspective. *J. Mater. Sci.* **36**, 3143–3164 (2001).
15. Eggleston, J. J., McFadden, G. B. & Voorhees, P. W. A phase-field model for highly anisotropic interfacial energy. *Physica D* **150**, 91–103 (2001).
16. Allen, L., Beijersbergen, M. W., Spreeuw R. J. C. & Woerdman, J. P. Orbital angular-momentum of light and the transformation of Laguerre-Gaussian laser modes. *Phys. Rev. A* **45**, 8185–8189 (1992).
17. Sekhar, J. A. & Trivedi, R. Solidification microstructure evolution in the presence of inert particles. *Mater. Sci. Eng. A* **147**, 9–21 (1991).
18. Rohatgi, P. K., Pasciak, K., Narendranath, C. S., Ray, S. & Sachdev, A. Evolution of microstructure and local thermal conditions during directional solidification of A356-SiC particle composites. *J. Mater. Sci.* **29**, 5357–5366 (1994).
19. Dutta, B. & Surappa, M. K. Directional dendritic solidification of a composite slurry: Part I. Dendrite morphology. *Metall. Mater. Trans. A* **29**, 1319–1327 (1998).
20. Dutta, B. & Surappa, M. K. Directional dendritic solidification of a composite slurry: Part II. Particle distribution. *Metall. Mater. Trans. A* **29**, 1329–1339 (1998).

### Acknowledgements

This work has been supported by contracts OTKA-T-037323, ESA Prodex 14613/00/NL/SFe, and ESA MAP Project No. AO-99-101. The authors would like to thank W. J. Boettinger for his helpful comments and criticism.

Correspondence and requests for materials should be addressed to L.G.

### Competing financial interests

The authors declare that they have no competing financial interests.